Introduction

In seismics, interferometry is used to turn receivers of passive or active measurements into sources, without knowing the velocity model. Interferometry can be done as a trace to trace process using Cross-Correlations or by a multidimensional deconvolution (MDD) approach, where arrays of sources and receivers are used. An overview of interferometry can be found in Wapenaar et al. (2008a) or in Schuster (2009).
In this research, interferometry by MDD is applied to a synthetic marine Controlled-Source Electromagnetic (CSEM) dataset. As stated above, the sources are redatumed to the receiver locations during this process. Additionally, the direct field is removed and the material parameters above the receivers are homogenized. For CSEM this means, that all effects related to the air-water interface are removed (Wapenaar et al., 2008b).
Hunziker et al. (2009) showed, that the spatial receiver sampling for a successful implementation of interferometry by MDD in CSEM, is dependent on the vertical source-receiver distance. Their rule stated, that the receiver spacing has to be equal to or smaller than the vertical source-receiver distance. This research shows, how their sampling criteria can be relaxed using elongated sources and what the limitations of such sources are.

Theory

Interferometry by MDD consists basically of two steps: First the multicomponent data need to be decomposed into upwards- and downwards-decaying fields, $\hat{\mathbf{P}}^-$ and $\hat{\mathbf{P}}^+$, respectively, which can be related to each other through the reflection response $\hat{\mathbf{R}}_0^+$. The superscript $^+$ indicates, that this is a response due to a downwards decaying field and the subscript $_0$ denotes that no multiples from above the receiver level are included. In matrix notation (Berkhout, 1982), this relation is given by:

$$\hat{\mathbf{P}}^- = \hat{\mathbf{R}}_0^+ \hat{\mathbf{P}}^+, \tag{1}$$

where the hat denotes space-frequency domain. Each column of the matrices contains various receiver positions for a fixed source position, while for the rows the situation is reversed. The second step, solves equation 1 for $\hat{\mathbf{R}}_0^+$. This can for example be done in a least-squares sense

$$\hat{\mathbf{R}}_\mathbf{0}^+ = \hat{\mathbf{P}}^- \left(\hat{\mathbf{P}}^+\right)^\dagger \left[\hat{\mathbf{P}}^+ \left(\hat{\mathbf{P}}^+\right)^\dagger + \varepsilon^2 \mathbf{I}\right]^{-1}. \tag{2}$$

The superscript † denotes complex-conjugation and transposition and $\mathbf{I}$ is the identity matrix. The stabilization parameter ε prevents the inversion from getting unstable. The retrieved $\hat{\mathbf{R}}_0^+$ is the field with a source at the receiver level, without a direct field and with the water layer replaced with a homogeneous halfspace consisting of the same material as the first layer below the water.

Modeling

2D TM-mode synthetic data were modeled for a very dense receiver array at the ocean bottom, consisting of 4096 receivers separated by 2.5 m. The receivers record the inline electric field E_x and the crossline magnetic field H_y. The source is a point-source, has a frequency of 0.5 Hz and is situated 25 m above the receivers. The 1D Earth structure consists, from top to bottom, of a halfspace of air, a water layer and a halfspace of sediments, which is intersected by a reservoir layer. The precise geometry and electromagnetic parameters are shown in Figure 1.
The recorded fields are shown in the space-domain in Figures 2a and b, and in the wavenumber-domain in Figures 2d and e. In this ideal setup, the reflection response is retrieved perfectly (Figures 2c and f). The large bandwidth of the original data (Figures 2d and e) demands the very dense sampling, which is necessary to successfully decompose the recorded fields (Hunziker et al., 2009). On the other hand, the retrieved reflection response, which contains only information about the subsurface, has a much narrower bandwidth (Figure 2f) and thus can be correctly sampled much sparser. Consequently, if the

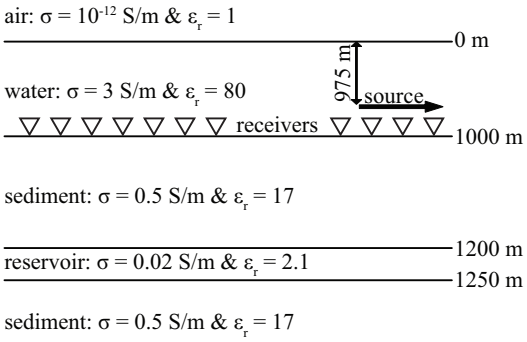

Figure 1 *Setup of numerical modeling: The black arrow indicates the source, white triangles the receivers. Conductivity σ and relative permittivity ε_r are given in the according layer.*

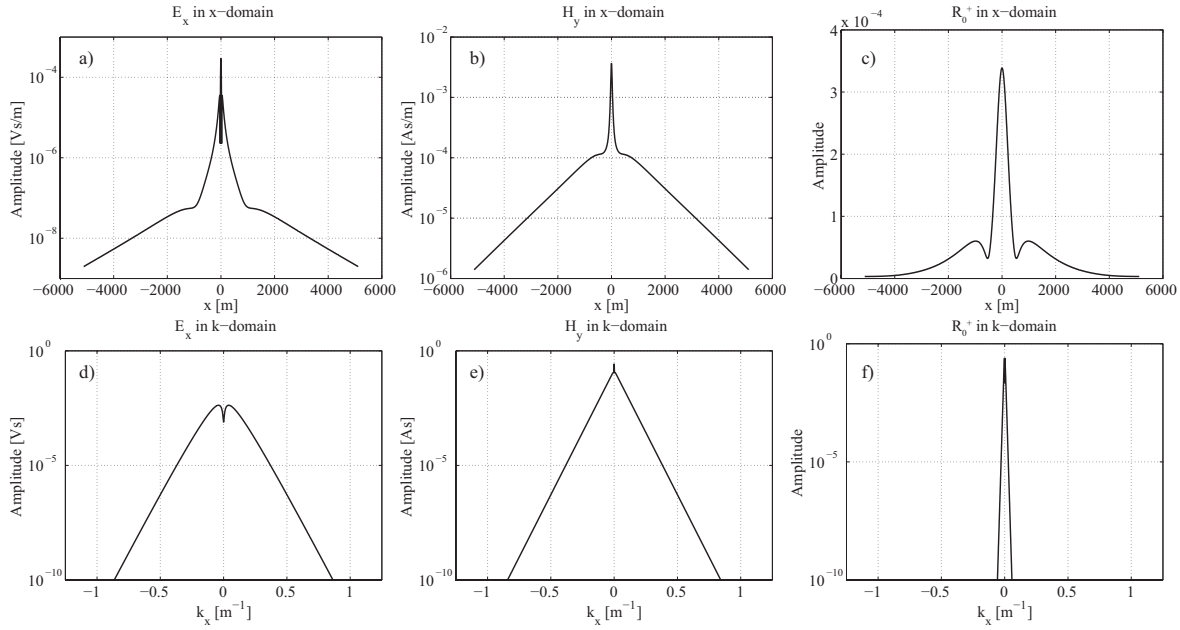

Figure 2 *a) Electric field in the space-domain, b) magnetic field in the space-domain, c) retrieved reflection response in the space-domain, d) electric field in the wavenumber-domain, e) magnetic field in the wavenumber-domain and f) retrieved reflection response in the wavenumber-domain.*

bandwidth of the data can be limited in some way, the sampling criteria can be relaxed, without losing information about the subsurface. A way to reduce the bandwidth of the data is the usage of elongated sources.

Results

Elongated sources of different lengths are created numerically, by a spatial convolution of the data with a boxcar-function. To test the effects of elongated sources on the spacing, the data are gradually sparsened by deleting every second sample. Figure 3 shows the reflection response retrieved from data created by a point-source for three different sampling distances. The directly modeled reflection response (black) is the correct solution. The blue and the red curves show retrieved reflection responses. The only difference between the blue and the red curve is, that the unstable tails of the upwards decaying field have been tapered prior to deconvolving for the red curve. With a spacing of 10 m (Figure 3a), the reflection response is retrieved perfectly, except some instabilities around zero offset, which can be eliminated through tapering of the upwards decaying field. Further increase of the spacing to 20 m (Figure 3b)

leads to growing instabilities around zero offset if no taper is applied. Otherwise the reflection response is retrieved well, besides a small underestimation of the amplitude of the sidelobes. The situation is completely different if the receiver spacing is increased to 40 m (Figure 3c). In that case, the tapered as well as the untapered retrieved reflection response are completely wrong. Consequently, the spacing is too large to correctly sample the data.

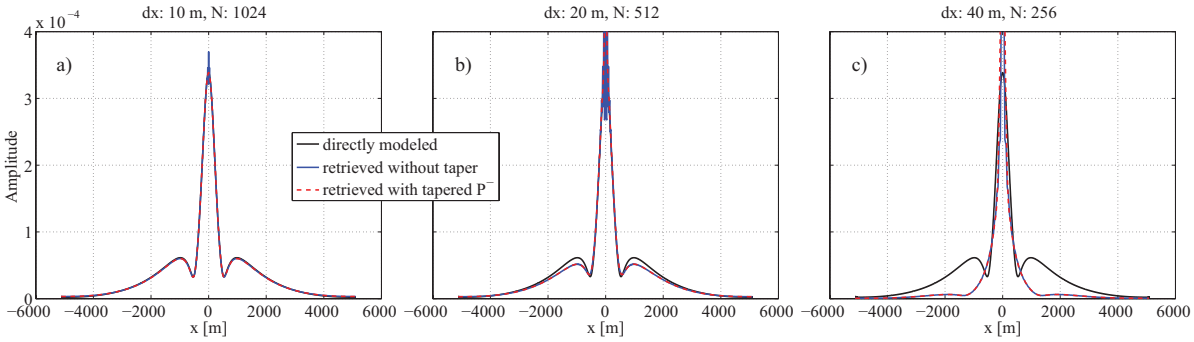

Figure 3 *Directly modeled reflection response (black), retrieved reflection response based on full upwards decaying field (blue) and retrieved reflection response based on tapered upwards decaying field (red) for receiver spacings of a) 10 m, b) 20 m and c) 40 m. The parameter N in the figure head gives the amount of samples.*

The reflection responses, plotted in Figure 4, are retrieved from data created by a source with a length of 80 m. Figure 4a shows the retrieved reflection responses for a spacing of 40 m. At this receiver spacing the reflection response could not be retrieved if the data were created by a point-source (Figure 3c). If a source of the length of 80 m is used, the reflection response can be retrieved well. There are instabilities around zero offset in the untapered case (blue curve), but with a tapered upwards decaying field, these instabilities vanish. However, in that case the amplitude around zero offset is not retrieved correctly. Since the overall shape of the reflection response is correct, this result is considered as a successful retrieval. This is also the case for a receiver spacing of 80 m (Figure 4b). Again, instabilities in the retrieved reflection response can be eliminated by tapering the upwards decaying field. A further increase of the receiver spacing to 160 m (Figure 4c) leads to a incorrectly retrieved reflection response. The largest possible receiver spacing, with which the reflection response can still be retrieved well, was

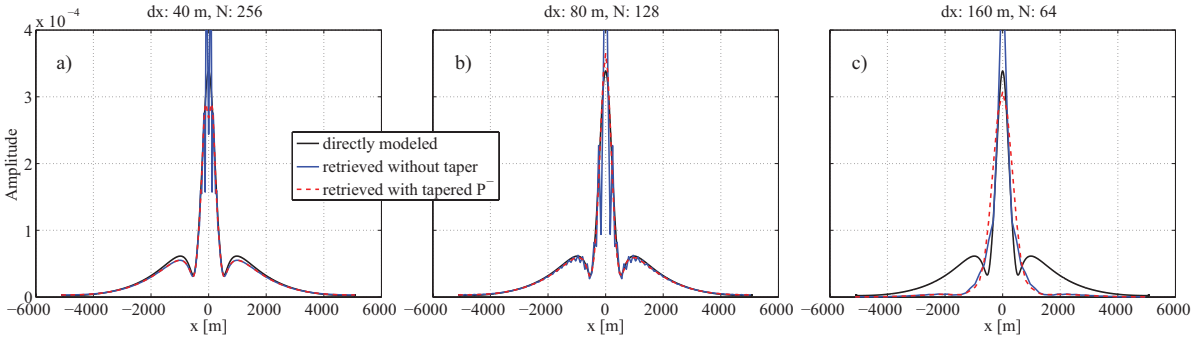

Figure 4 *Same as Figure 3, but this time a source with a length of 80 m was used. The reflection responses are shown for receiver spacings of a) 40 m, b) 80 m and c) 160 m.*

determined for different source lengths as well as different vertical source-receiver distances (source heights) by visual inspection as shown in Figure 5. It can be seen, that the larger of the two parameters (source length or source height) determines the largest possible sampling distance. The receiver-sampling has to be equal or smaller than that parameter. The taper brings only an improvement for

source heights smaller or equal than 100 m. There are no instabilities for larger source heights and therefore a taper is not necessary. In contrary, the taper even degrades the result by affecting the amplitude. For source lengths larger than 160 m, the taper leads to a broadening of the reflection response for large sampling distances. Therefore, for small source heights and large source lengths, the general shape of the reflection response can be retrieved with the sampling distances indicated in Figure 5, but the locations of the local minima are shifted to larger offsets. For larger source heights, the taper can be omitted, and therefore larger sampling distances can be applied also for larger source lengths without retrieving a broadened reflection response.

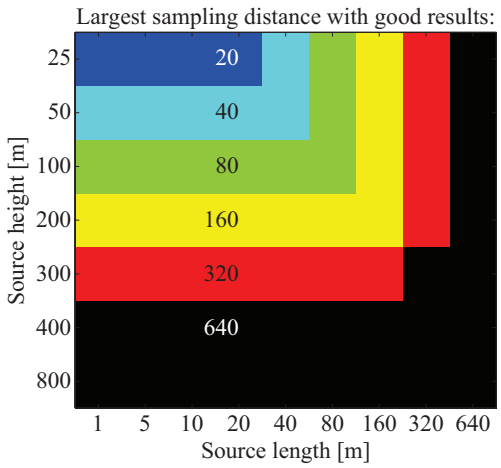

Figure 5 *Largest possible receiver spacing, with which the reflection response can be retrieved well, as a function of source length and source height. The colors indicate the receiver spacing in meters.*

Conclusions

The strict receiver-sampling criteria introduced by Hunziker et al. (2009) can be relaxed if the bandwidth of the data is limited through the usage of elongated sources. It has been shown, that the larger of the two parameters, source length or source height, determines the largest possible receiver sampling. To overcome instabilities in the retrieved reflection response, a taper is applied to the upgoing field for vertical source-receiver distances smaller or equal than 100 m.

Acknowledgements

This research is supported by the Dutch Technology Foundation STW, applied science division of NWO and the Technology Program of the Ministry of Economic Affairs.

References

Berkhout, A. J. [1982] *Seismic Migration. Imaging of Acoustic Energy by Wave Field Extrapolation.* Elsevier.

Hunziker, J., Slob, E., and Wapenaar, K. [2009] Controlled source electromagnetic interferometry by multidimensional deconvolution: spatial sampling aspects in sea bed logging. *71st EAGE Conference and Exhibition, Expanded Abstracts.*

Schuster, G. [2009] *Seismic Interferometry.* Cambridge University Press.

Wapenaar, K., Draganov, D. and Robertsson, J.O.A. [2008a] *Seismic Interferometry: History and Present Status.* Society of Exploration Geophysicists, Geophysics Reprint Series No. 26.

Wapenaar, K., Slob, E. and Snieder, R. [2008b] Seismic and electromagnetic controlled-source interferometry in dissipative media. *Geophysical Prospecting*, **56**, 419-434.